Research article

The root cortex cell hydraulic conductivity is enhanced with increasing chromosome ploidy in wheat

Weifeng Wang [a,c,1], Xiaoqing Yang [a,c,1], Suiqi Zhang [a,b,*], Yingying Sun [b]

[a] State Key Laboratory of Soil Erosion and Dryland Farming on the Loess Plateau, Institute of Soil and Water Conservation, Chinese Academy of Sciences and Ministry of Water Resources, Yangling, Shaanxi 712100, PR China
[b] Northwest A&F University, Yangling, Shaanxi 712100, PR China
[c] University of Chinese Academy of Sciences, Beijing 100049, PR China

ABSTRACT

Wheat (*Triticum* spp.) root water uptake is enhanced with increasing chromosome ploidy, but the underlying mechanism is unclear. The leaf transpiration rate (E), individual root (Lp_r) and cortical cell (Lp_c) hydraulic conductivity, cortical cell volume (V_c) and transcription levels of two putative plasma intrinsic aquaporin genes (*PIPs*) were investigated in wheat seedlings with different chromosome ploidy (*Triticum monococcum* (2X, AA); *Triticum dicoccum* (4X, BB); *Triticum aestivum* (6X, AABBDD)). The E, Lp_r and Lp_c of wheat increased with increasing ploidy, but the V_c was reduced. Osmotic stress significantly reduced the E, Lp_c, Lp_r, and the relative mRNA content of *TaPIP1;2* and *TaPIP2;5* in wheat. Under both well-watered and osmotic stress conditions, the Lp_r was significantly and positively correlated with the E and Lp_c, and the relative mRNA content of *TaPIP1;2* and *TaPIP2;5* was significantly and positively correlated with Lp_c and Lp_r, respectively. For well-watered or osmotically stressed wheat plants, the Lp_c was reduced, but the Lp_c/Lp_r increased with increasing V_c, suggesting that V_c affects root radical water transport. Thus, the increased Lp_c and transcription levels of *TaPIP1;2* and *TaPIP2;5* in wheat roots provides insight into the mechanisms underlying enhanced root water uptake with increasing chromosome ploidy during wheat evolution.

1. Introduction

Plant growth depends on an optimum balance between water uptake in the roots and water losses through the shoots. In the past decades, the physiological and morphological responses of crops to soil water shortage have been studied to reduce shoot transpiration [1,2], and deficit irrigation has been an important approach to reduce water use and improve water use efficiency in agriculture [3,4]. However, the roots typically provide the water input in whole-plant water balance and, hence, play a central role in maintaining the plant water status in a changing water environment [5]. Due to technical problems, the basic hydraulic properties of roots are not yet adequately understood [6]. Based on the results obtained from early anatomical and experimental studies using root and cell pressure probes, a composite model of water transport in roots was proposed [7]. The model postulates that water moves across plant tissues through both apoplastic and cell-to-cell pathways. The cell-to-cell pathway refers to water flow through the plasmodesmata and/or across membranes, substantially contributing to whole-plant hydraulic resistance [8]. Peter Agre et al. identified aquaporins (AQPs), which substantially changed the understanding of the water trans-membrane movement mechanism [9] and provided a molecular basis for plant water transport and regulation.

AQPs are biological membrane structures belonging to the major intrinsic protein (MIP) superfamily [10]. AQPs have been divided into four or five subfamilies, and the plasma membrane intrinsic proteins (PIPs) are primarily located in the plasma membrane [11,12]. PIPs can be further subdivided into PIP1 and PIP2 groups [13]. In contrast with PIP1 proteins, the overexpression of PIP2 proteins considerably increased the water permeability of oocyte membranes [14,15]. However, the coexpression of PIP1;2 and some
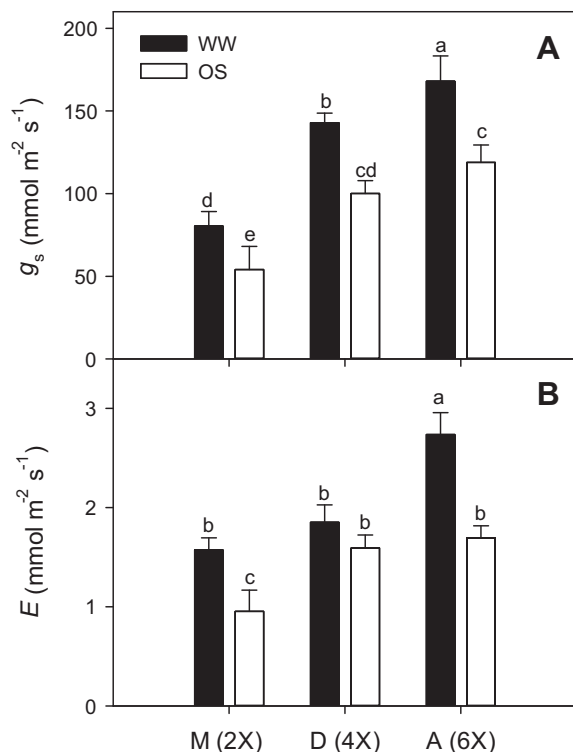
Fig. 1. Leaf stomatal conductance (g_s; A) and transpiration rate (E; B) in wheat. M (2X) represents *Triticum monococcum*, D (4X) represents *T. dicoccum* and A (6X) represents *T. aestivum*. The black columns (WW) indicate the well-watered plants, and the open columns (OS) indicate the osmotically stressed plants. The error bars indicate the S.D. from six plants. The lower case letters indicate the significant differences at $P < 0.05$.

PIP2 isoforms further increased the water permeability of oocyte membranes [16], indicating the roles of PIP proteins in regulating water permeability through the formation of heterologous tetramers. Studies have implicated a role for PIPs in regulating leaf and root hydraulic properties. PIPs have been isolated from cells in the root cortex, root endodermis, leaf xylem parenchyma and bundle sheath in plants [17,18]. PIP1 or PIP2 antisense lines exhibited reduced root hydraulic properties and recovered more slowly after rewatering than wild-type lines [19,20]. Diurnal variations in the root hydraulic conductivity of *Lotus japonicus* and maize (*Zea mays* L.) have been associated with the expression of some aquaporins, particularly PIP2 [21,22]. However, in grapevine (*Vitis vinifera*), the increased expression of *PIP1;1* reflected diurnal variation in the root system and cortical cell hydraulic conductivity (Lp_c) in response to water stress, while the expression of *PIP2;2* did not change [23]. Furthermore, PIP1;2 and PIP2;5 have been associated with cell membrane and/or root hydraulic conductivity in *Oryza sativa* [24], *Arabidopsis* [25], and maize [26]. Zhang and Tyerman [27] reported that HgCl$_2$ largely inhibited the Lp_c of wheat, which suggests a role

for aquaporins in cortex cell hydraulics. *TaPIP1;2* and *TaPIP2;5* have been identified in wheat, and the sequences of these genes have been submitted to the NCBI sequence database [28]. However, there are few studies concerning the relationships between *TaPIP1;2* and *TaPIP2;5* and root hydraulic traits in wheat (*Triticum* spp.).

Many cereal grasses, such as wheat, have complex genomes with several genotypes: diploid, tetraploid and hexaploid species. Wheat has been cultivated for over 10,000 years and has become one of the most important cereal crops worldwide [29]. In China, wheat accounts for 22–27% of total crop sown area in the past decade [30]. Thus, characterizing the photosynthetic features and water use efficiency of wheat has garnered much attention in scientific research [31–33]; however, root water uptake in wheat has received much less attention. Zhao et al. showed that the root system (Lp_{rs}) and individual root (Lp_r) hydraulic conductivity increased with increasing chromosome ploidy (2X → 6X) [34], thereby enhancing root water uptake with increased ploidy. However, changes in the Lp_c of wheat with increased ploidy have not been reported.

We hypothesize that the Lp_c of wheat increases with increasing ploidy, and the expression of *TaPIP1;2* and *TaPIP2;5* is associated with root hydraulic traits. To confirm this hypothesis, we selected three wheat cultivars with differing ploidy classes (*Triticum monococcum* (M; 2X); *Triticum dicoccum* (D; 4X); *Triticum aestivum* (A; 6X)) based on our former research [34]. The Lp_r, Lp_c and expression of *TaPIP1;2* and *TaPIP2;5* transcripts in wheat seedlings under two water supply conditions were examined. In this study, we reveal the relationships between Lp_r, Lp_c, gene transcription, cortex cell volume and leaf water status in wheat plants.

2. Results

2.1. Leaf gas exchange in different ploidy classes of wheat

For well-watered plants, the leaf transpiration rate (E) and stomatal conductance (g_s) ranged from 1.57 to 2.74 mmol m^{-2} s^{-1} and 80 to 160 mmol m^{-2} s^{-1}, respectively (Fig. 1A and B). The E and g_s of well-watered plants increased with increasing chromosome ploidy. The osmotic stress induced with 10% PEG6000 significantly reduced the E (40%) and g_s (30%) in the three wheat cultivars, except for the E of *T. dicoccum*, which was not significantly different from that of well-watered and osmotically stressed plants (Fig. 1). The E and g_s of osmotically stressed plants also increased with increasing chromosome ploidy (Fig. 1).

2.2. Anatomical and morphological changes

Fifteen days after germinating, no matter well-watered or osmotically stressed plants, the seminal roots of three wheat cultivars had similar anatomical structure: 5 or 6 cortical cell layers, 6 or 7 mature early metaxylem vessels, only one immature later metaxylem and no Casparian bands in the endodermis (see

Table 1

The anatomic parameters of seminal roots and morphologic parameters of wheat under osmotic stress conditions. M (2X) represents *Triticum monococcum*, D (4X) represents *T. dicoccum* and A (6X) represents *T. aestivum*. WW indicates the well-watered plants, and OS indicates the osmotically stressed plants. Mean ± S.D. are shown and the lower case letters indicate the significant differences at $P < 0.05$. The figure in parenthesis indicates the number of replications.

Cultivars	Treatments	Length of cortical cells (μm)	Diameter of cortical cells (μm)	Volume of cortical cells (10^5 μm)	Total root length per plant (cm)	Total leaf length per plant (cm)	Ratio of root surface area to leaf area
M (2X)	WW	267 ± 53 a (46)	46.4 ± 5.3 a (46)	4.52 ± 0.86 a (46)	146 ± 21 bc (15)	49.4 ± 5.2 c (15)	1.91 ± 0.17 c (15)
	OS	215 ± 36 b (48)	42.8 ± 4.0 a (48)	3.11 ± 0.78 c (48)	117 ± 11 d (13)	41.5 ± 3.6 d (13)	2.61 ± 0.38 a (13)
D (4X)	WW	218 ± 31 b (52)	47.2 ± 4.7 a (52)	3.81 ± 0.74 b (52)	155 ± 17 b (11)	57.1 ± 6.6 b (11)	1.41 ± 0.27 d (11)
	OS	182 ± 37 c (53)	45.8 ± 4.3 a (53)	2.95 ± 0.55 cd (53)	126 ± 11 cd (14)	45.0 ± 5.5 cd (14)	2.09 ± 0.38 bc (14)
A (6X)	WW	188 ± 32 c (37)	45.8 ± 3.7 a (37)	2.85 ± 0.56 de (37)	271 ± 25 a (14)	70.1 ± 6.4 a (14)	1.73 ± 0.21 cd (14)
	OS	174 ± 30 c (39)	43.9 ± 4.6 a (39)	2.52 ± 0.52 e (39)	259 ± 41 a (13)	60.3 ± 4.1 b (13)	2.42 ± 0.33 ab (13)

examples in Supplementary data Figures A.1 and A.2). Under osmotic stress, the length of cortical cells was significantly reduced in the seminal roots of *T. monococcum* and *T. dicoccum* while the diameter of cortical cells of the three cultivars had no significant changes, which contributed to the significantly reduced V_c in *T. monococcum* and *T. dicoccum* (Table 1). The total root or leaf length per plant of three wheat cultivars was significantly reduced by osmotic stress except the root length of *T. aestivum*. The ratio of root surface area to leaf area of osmotically stressed plants was significantly higher than that of well-watered plants (Table 1).

2.3. Hydraulic conductivity measurements

For well-watered plants, the individual root hydraulic conductivity (Lp_r) in wheat, measured using a root pressure probe, ranged from 8.5 to 19.6 · 10^{-7} m s^{-1} MPa^{-1} (Fig. 2A). Osmotic stress significantly reduced the Lp_r of the three wheat cultivars (31–38%). The Lp_r of well-watered or osmotically stressed plants increased with increasing chromosome ploidy (Fig. 2A). Similarly, the root cortex cell hydraulic conductivity (Lp_c) in wheat was also increased. For well-watered plants, the Lp_c ranged from 7.8 to 11.2 · 10^{-7} m s^{-1} MPa^{-1} and increased with increasing ploidy. The Lp_c of osmotically stressed plants was significantly reduced (20%) to a value lower than that of well-watered plants (Fig. 2B). The data obtained from well-watered plants and plants under osmotic stress showed significantly positive relationship between Lp_r, E ($R^2 = 0.882$; $P = 0.006$) (Fig. 3A) and Lp_c ($R^2 = 0.979$; $P = 0.0002$) (Fig. 3B).

The cortical cell volume (V_c) of wheat was reduced with increasing ploidy from diploid to hexaploid genotypes. Osmotic stress significantly reduced the V_c of *T. monococcum* and *T. dicoccum*, but not that of *T. aestivum* (Table 1). The correlation
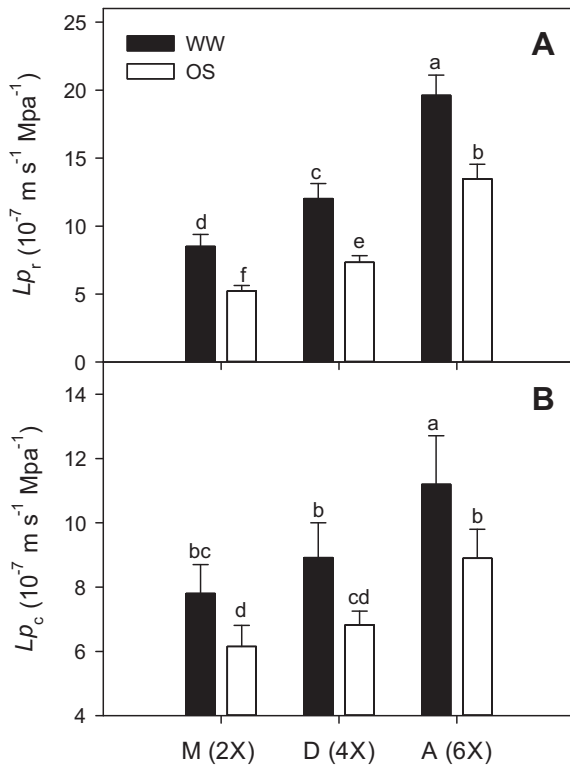
Fig. 2. Individual root (Lp_r; A) and cortex cell (Lp_c; B) hydraulic conductivities in wheat. M (2X) represents *Triticum monococcum*, D (4X) represents *T. dicoccum* and A (6X) represents *T. aestivum*. The black columns (WW) indicate the well-watered plants, and the open columns (OS) indicate the osmotically stressed plants. The error bars indicate the S.D. from 11 to 15 plants, and the lower case letters indicate the significant differences at $P < 0.05$.
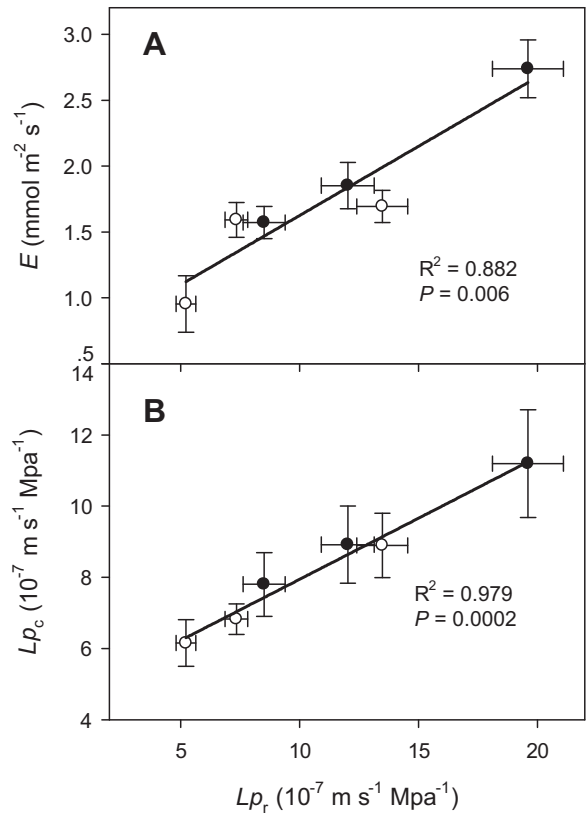
Fig. 3. Correlations between the individual root hydraulic conductivity (Lp_r) and the leaf transpiration rate (E; A) or cortex cell hydraulic conductivity (Lp_c; B). Points are the mean of parameters and error bars represent the S.D. (for E, $n = 6$; for Lp_r and Lp_c, $n = 11$–15). The black circles indicate the well-watered cultivars, and the open circles indicate the osmotically stressed cultivars. The correlation analyses were performed using SigmaPlot version 12.0, and the relation coefficient (R^2) and significant level (P) are shown.

analysis showed that the Lp_c in wheat was significantly and negatively correlated with the V_c for well-watered plants ($P = 0.022$), but not for osmotically stressed plants ($P = 0.080$; Fig. 4A). The ratio of Lp_c to Lp_r (Lp_c/Lp_r) may suggest the relative contribution of the cell-to-cell pathway to root radial water transport. The Lp_c/Lp_r increased with increasing V_c, under both well-watered and osmotic stress conditions (Fig. 4B).

2.4. Relative mRNA content of TaPIPs

PIPs have been implicated in the regulation of cell membrane water permeability and root hydraulic conductivity. To obtain evidence of this function in wheat, the relative mRNA content of *TaPIP1;2* and *TaPIP2;5* was measured in the roots using real-time PCR. For well-watered plants, the relative *TaPIP1;2* and *TaPIP2;5* mRNA content increased in the roots of wheat plants with increasing ploidy (Fig. 5A and B). Osmotic stress significantly reduced the relative mRNA levels of *TaPIP1;2* and *TaPIP2;5* in wheat roots, and the reduction of *TaPIP2;5* (55–77%) transcription levels in osmotically stressed plants was greater than that of *TaPIP1;2* (20–44%). Thus, the correlation analyses revealed a significantly positive relationship between the relative mRNA levels of *TaPIP1;2* and *TaPIP2;5* and the Lp_r and Lp_c, respectively (Fig. 6A–D).

3. Discussion

Clarifying the mechanisms underlying root water uptake is important to understand whole-plant water balance and improve
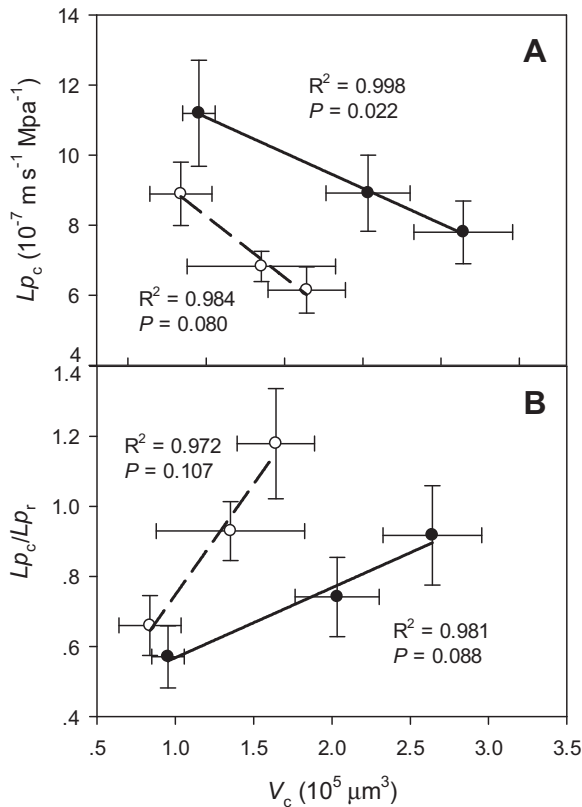
Fig. 4. Correlations between the root cortex cell hydraulic conductivity (Lp_c; A) or the ratio of cortex cell hydraulic conductivity to individual root hydraulic conductivity (Lp_c/Lp_r; B) and cortex cell volume (V_c) in wheat. Points are the mean of parameters and error bars represent the S.D. from 11 to 15 plants. The black circles indicate the well-watered cultivars, and the open circles indicate the osmotically stressed cultivars. The correlation analyses were performed using SigmaPlot version 12.0, and the relation coefficient (R^2) and significant level (P) are shown.

water use efficiency in wheat. Using wheat plants with different ploidy levels, we investigated leaf transpiration, individual root and cortex cell hydraulic conductivities and the transcription levels of *TaPIP1;2* and *TaPIP2;5*. Based on these results and the data obtained from previous studies, some questions and hypotheses concerning root water uptake will be discussed.

3.1. Leaf water status regulates root hydraulic conductivity?

To assimilate CO_2, leaf stomata open and induce transpiration. The interactions between Lp_r and E are complex, and the explanations for these interactions are paradoxical [5]. Positive correlations between Lp_r and E have been observed in grapevine [23], *Medicago sativa* [35] and maize [36]. In this study, the Lp_r and E of polyploid wheat showed a significantly positive relationship (Fig. 3A). For well-watered plants under constant conditions, the Lp_r increased with increasing E among polyploid wheat species (Fig. 3B). This result might reflect the dependence of Lp_r on E [37]. However, the osmotic gradient in wheat roots could change in response to PEG-induced osmotic stress. For example, the transcription levels of *TaPIP1;2* and *TaPIP2;5* were down-regulated (Fig. 5A and B), potentially contributing to the significant reduction of Lp_c (Fig. 2B). Lp_c and Lp_r showed a significantly positive relationship (Fig. 3B) and indicated the root water uptake at two scale levels. Thus, it is reasonable to conclude that a reduction in the root water supply would also reduce the E (Fig. 1B). The results of the present study showed correlations between the Lp_r and E in wheat in which changes that affect one factor can also affect the other during
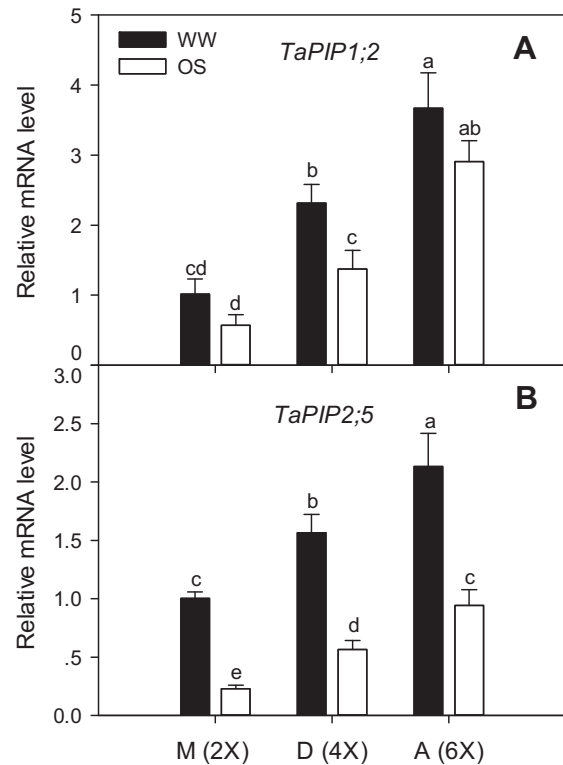

Fig. 5. Relative mRNA content of *TaPIP1;2* (A) and *TaPIP2;5* (B) in the roots of wheat plants. M (2X) represents *Triticum monococcum*, D (4X) represents *T. dicoccum* and A (6X) represents *T. aestivum*. The black columns (WW) indicate the well-watered plants, and the open columns (OS) indicate the osmotically stressed plants. The error bars represent the S.D. from three sample replications, and each sample was obtained from two plants. The lower case letters indicate the significant differences at $P < 0.05$.

different water supply conditions. Thus, high leaf transpiration requires enhanced root water uptake to maintain whole-plant water balance during wheat evolution. The two-way coordination of Lp_r and E indicates the water balance of root–shoot interactions.

3.2. Cortical cell volume effects root radial water flow pathway?

Steudle et al. proposed a composite transport model based on both anatomical and experimental data from the roots [6,7]. However, the effects of the cortical cell volume (V_c) on root water transport remain elusive. Using polyploid wheat, the results obtained in the present study suggested that the Lp_c increases with decreasing V_c, under well-watered or osmotic stress conditions (Fig. 4A). As the V_c of well-watered plants decreases, both the plasma membrane and cell wall area increases. In addition, the relative mRNA content of *TaPIP1;2* and *TaPIP2;5* also increased with decreasing V_c (Fig. 5A and B). Thus, both the cell-to-cell and apoplastic pathways increase with decreasing V_c, which might partly explain the increased Lp_r of higher ploidy wheat (Fig. 4). The Lp_c/Lp_r might partly indicate the relative contribution of the cell-to-cell pathway to root radical water transport. Therefore, when the Lp_r increases with increasing ploidy, the Lp_c/Lp_r is reduced with decreasing V_c, indicating an increased contribution of the apoplastic pathway (Fig. 4B). Thus, for well-watered polyploid wheat, a reduction in the V_c might explain an increase in root hydraulics.

During osmotic stress, the Lp_c and Lp_r of wheat were significantly reduced (Fig. 2A and B). Positive relationships among E, Lp_c and Lp_r were also observed during osmotic stress (Fig. 3A and B). However, Lp_c/Lp_r in osmotically stressed plants was higher than that in well-watered plants (Fig. 4B), suggesting an increased
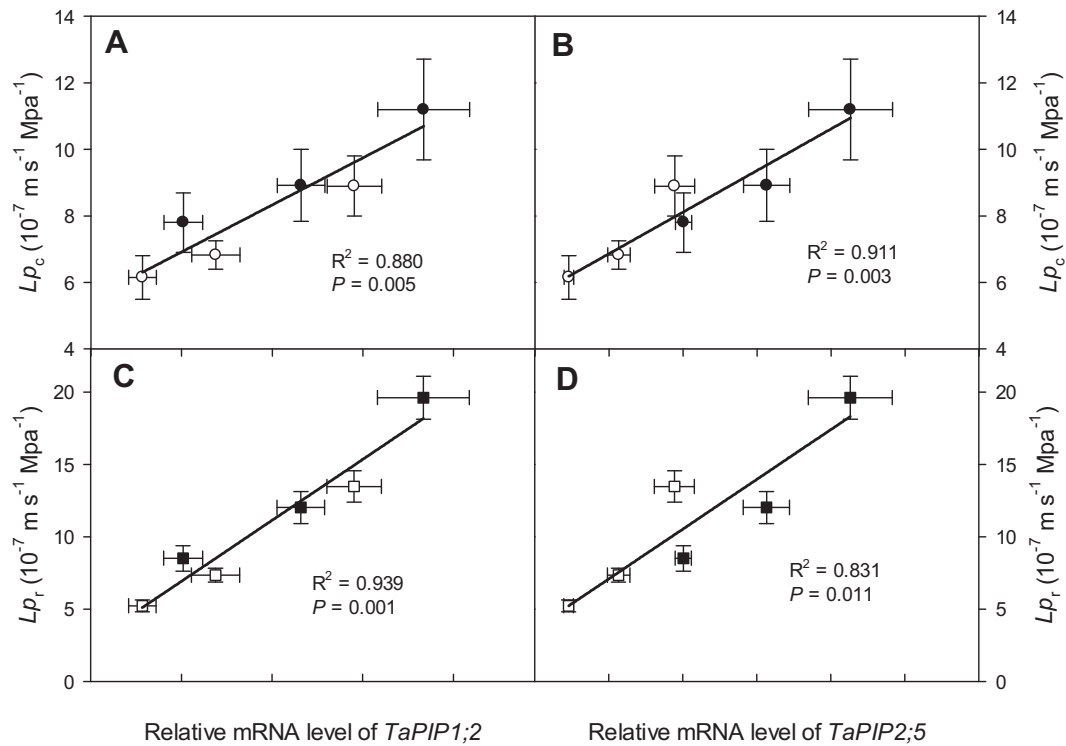
Fig. 6. Root cortex cell hydraulic conductivity (Lp_c) and individual root hydraulic conductivity (Lp_r) are positively correlated with the relative mRNA content of *TaPIP1;2* and *TaPIP2;5*, respectively, in the roots. Points are the mean of parameters and error bars represent the S.D. (Lp_c and Lp_r, $n = 11-15$; relative mRNA levels, $n = 3$). The black circles indicate the well-watered plants, and the open circles indicate the osmotically stressed plants. The correlation analyses were performed using SigmaPlot version 12.0, and the relation coefficient (R^2) and significant level (P) are shown.

contribution of the cell-to-cell pathway. This result is consistent with the composite transport model [6]. Leaf transpiration was reduced during osmotic stress (Fig. 1B); thus, a reduction in the hydrostatic gradient might accompany a reduction in the contribution of the apoplastic pathway.

3.3. Two TaPIPs expression in wheat with different ploidy levels

With increased chromosome ploidy in wheat (2X → 6X), the whole-root system and individual root water uptake are enhanced [34]. In the present study, the Lp_c of wheat was also enhanced with increased ploidy (Fig. 2B) and showed a significantly positive relationship with Lp_r (Fig. 3B). PIPs have been implicated in the regulation of root hydraulic resistance [10], and important roles of PIP1;2 and PIP2;5 have been demonstrated in rice [24], maize [26] and *Arabidopsis* [25]. Therefore, we measured the transcription levels of *TaPIP1;2* and *TaPIP2;5* in polyploid wheat roots. The data showed that the transcription levels of *TaPIP1;2* and *TaPIP2;5* increased with increasing ploidy (Fig. 5) and demonstrated significantly positive correlations with Lp_c and Lp_r (Fig. 6) under both well-watered and osmotic stress conditions. Notably, *TaPIP1;2* and *TaPIP2;5* have only been identified through gene isolation and sequence homology [28], and direct experimental data concerning the functions of TaPIP1;2 and TaPIP2;5 in water permeability have not been reported. However, based on the data obtained from previous studies and the results obtained here, TaPIP1;2 and TaPIP2;5 play important roles in the root hydraulics of wheat.

4. Conclusion

Using wheat plants with different ploidy levels, we showed that leaf transpiration, individual root and cortical cell hydraulic

conductivities and the transcription levels of *TaPIP1;2* and *TaPIP2;5* increased with increasing ploidy. The Lp_c was significantly correlated with the Lp_r, and the cortical cell volume might affect the contribution of the cell-to-cell pathway in root radical water transport. The transcription levels of *TaPIP1;2* and *TaPIP2;5* were correlated with Lp_c and Lp_r. Taken together, these results confirmed our hypothesis and might explain the enhanced root water uptake observed with increasing ploidy in wheat plants.

5. Martial and methods

5.1. Plant material and treatments

The wheat seeds (*T. monococcum* (2X, AA); *T. dicoccum* (4X, AABB); *T. aestivum* (6X; cv: Shaan253, AABBDDD)) were disinfected using 2% sodium hypochlorite, rinsed with distilled water, and placed on moist filter paper for 2 days at 25 °C in a dark chamber for germinating. The seedlings were raised hydroponically in a growth chamber under a 12/12 h photoperiod (25/18 °C; RH 50–60%; 400 μmol photons m^{-2} s^{-1}). Half-strength modified Hoagland's nutrient solution (pH 6.0) was used for well-watered plants and osmotic stress was induced using nutrient solution with 10% PEG6000 (−0.30 MPa). And the mediums were well aerated using aquarium diffusers. Measurements were taken at the third leaf stage which was fifteen days after germinating.

5.2. Leaf gas exchanges

The leaf transpiration rate (E) and stomatal conductance (g_s) were measured from the middle of third leaf using an Li-6400 portable gas exchange system (LI-COR Inc., Lincoln, USA) between 10:30 and 11:30 AM. Six random plants were used in each measurement.

5.3. Morphological and anatomical parameters

The total root length, total leaf length, leaf area and root surface area were obtained with a scanner (Epson Perfection V700, Seiko Epson Crop., Suwa, Japan) and analyzed with WinRHIZO (Regent Instrument Inc., Quebec, Canada), and then the ratio of root surface area to leaf area was calculated. The length and diameter of cortical cells were measured with Image-Pro-Express 6.0 after pictures of cortical cells were taken under 10 × 40 optical microscope. Then the volume of cortical cells was simply calculated as cylinders.

5.4. Root hydraulic conductivity

The individual root hydraulic conductivity (Lp_r) of primary seminal roots was measured *in vitro* using a root pressure probe as detailed in previously published methods [38]. Briefly, to avoid the effects of lateral roots, 5 cm long root segments from the root apex were cut and connected to a root pressure probe. Root pressure can become steady 3–4 h after attachment and often ranges from 0.07 MPa to 0.12 MPa for wheat cultivars. The Lp_r was evaluated using hydrostatic root pressure relaxation tests. The root segment surface area (A_r) was calculated using the diameter and length of the root segment. The water exchange half time ($T_{1/2}^W$) was measured, and subsequently the Lp_r was calculated using the following formula:

$$Lp_r = \frac{\ln(2)}{A_r \times T_{1/2}^W \times \frac{\Delta P}{\Delta V}} \tag{1}$$

5.5. Cortex cell hydraulic conductivity

The root cortical cell hydraulic conductivity (Lp_c) was measured using a cell pressure probe as detailed in previously published methods [38]. The measurements were obtained from the 4 to 6 cortex cell layers at 2–3 cm from the root apex. Briefly, the elastic module (ε_c) was calculated from the cell volumes (V_c), and the changes in cell turgor (ΔP) was calculated from the changes in the cell volumes (ΔV) using the following formula:

$$\varepsilon_c = V_c \times \frac{dP}{dV} \approx V_c \times \frac{\Delta P}{\Delta V}. \tag{2}$$

The Lp_c was calculated from the cell sap osmotic pressure (π^i) and water exchange half time ($T_{1/2}^W$),

$$Lp_c = \frac{V_c}{A_c} \times \frac{\ln(2)}{T_{1/2}^W \times (\varepsilon_c + \pi^i)}. \tag{3}$$

Here, A_c represents the cortex cell surface area, which was calculated from the diameter and length of the cylindrical cortex cells.

5.6. Quantitative real-time PCR

The root segments (1–5 cm long from apex) were sampled at 11:00 AM for mRNA quantification. Three biological replications were conducted, and each replication was obtained from three plants. The samples were immediately immersed in liquid nitrogen and stored at −70 °C. Total RNA was extracted from the samples using an RNAprep pure Plant Kit (TIANGEN, Beijing, China). The RNA extract was digested with DNase I and examined using a dissociation curve to ensure that DNA was eliminated. The cDNA was synthesized *in vitro* using a TIANScript RT Kit (TIANGEN, Beijing, China) according to the manufacturer's instructions. The data for the relative mRNA content of *TaPIP1;2* (GI: 161897609) and *TaPIP2;5* (GI: 161897629) were evaluated against that for the internal reference genes *β-Actin* (GI: 48927617) and *α-Tubulin* (GI: 543383). Gene-specific primers (Supplementary Table A.1; synthesized by AuGCT, Beijing, China) and the Quant qRT-PCR (SYBR Green) Kit (TIANGEN, Beijing, China) were used for real-time PCR analysis. The PCR efficiency of each pair of primers was detected using a serial 10-fold dilution of cDNA. The PCR reaction, containing 0.5 μl of 20 μM primers, 15 μl of SYBR Green Master Mix, 0.5 μl of cDNA, and 8.5 μl of ddH$_2$O in a total volume of 20 μl, was performed in a DNA Engine Opticon (MJ Research, Waltham, USA) after the reactions were preheated at 95 °C for 30 s, followed by 40 cycles at 95 °C for 10 s, 62 °C for 30 s, and 72 °C for 30 s. The fluorescence data were collected at 72 °C, and the melting curve analysis was performed at 72 °C for 5 min, followed by heating to 95 °C at a rate of 0.5 °C s^{-1}. The data were calculated using the $2^{-\Delta\Delta Ct}$ method [39] and normalized against that of well-watered *T. monococcum* (2X) as a relative unit.

5.7. Statistical analysis

The means ± standard deviation (S.D.) are shown for each parameter. Student's *t*-test and Tukey's HSD test were performed in SPSS version 13.0. The correlation and regression analyses were conducted using SigmaPlot version 12.0.

Appendix A. Supplementary data

Supplementary data related to this article can be found at http://dx.doi.org/10.1016/j.plaphy.2013.03.021.

References

[1] W.J. Davies, S. Wilkinson, B. Loveys, Stomatal control by chemical signalling and the exploitation of this mechanism to increase water use efficiency in agriculture, New Phytologist 153 (2002) 449–460.

[2] N.C. Turner, Adaptation to water deficits: a changing perspective, Functional Plant Biology 13 (1986) 175–190.

[3] E. Fereres, M.A. Soriano, Deficit irrigation for reducing agricultural water use, Journal of Experimental Botany 58 (2007) 147–159.

[4] X.P. Deng, L. Shan, H. Zhang, N.C. Turner, Improving agricultural water use efficiency in arid and semiarid areas of China, Agricultural Water Management 80 (2006) 23–40.

[5] C. Maurel, T. Simonneau, M. Sutka, The significance of roots as hydraulic rheostats, Journal of Experimental Botany 61 (2010) 3191–3198.

[6] E. Steudle, Water uptake by roots: effects of water deficit, Journal of Experimental Botany 51 (2000) 1531–1542.

[7] E. Steudle, C.A. Peterson, How does water get through roots? Journal of Experimental Botany 49 (1998) 775–788.

[8] R.B. Heinen, Q. Ye, F. Chaumont, Role of aquaporins in leaf physiology, Journal of Experimental Botany 60 (2009) 2971–2985.

[9] G.M. Preston, T.P. Carroll, W.B. Guggino, P. Agre, Appearance of water channels in Xenopus oocytes expressing red cell CHIP28 protein, Science 256 (1992) 385–387.

[10] S. Tyerman, H. Bohnert, C. Maurel, E. Steudle, J. Smith, Plant aquaporins: their molecular biology, biophysics and significance for plant water relations, Journal of Experimental Botany 50 (1999) 1055–1071.

[11] U. Johanson, M. Karlsson, I. Johansson, S. Gustavsson, S. Sjovall, L. Fraysse, A.R. Weig, P. Kjellbom, The complete set of genes encoding major intrinsic proteins in *Arabidopsis* provides a framework for a new nomenclature for major intrinsic proteins in plants, Plant Physiology 126 (2001) 1358–1369.

[12] W. Park, B. Scheffler, P. Bauer, B.T. Campbell, Identification of the family of aquaporin genes and their expression in upland cotton (*Gossypium hirsutum* L.), BMC Plant Biology 10 (2010) 142–158.

[13] A. Weig, C. Deswarte, M.J. Chrispeels, The major intrinsic protein family of Arabidopsis has 23 members that form three distinct groups with functional aquaporins in each group, Plant Physiology 114 (1997) 1347—1357.

[14] F. Chaumont, F. Barrieu, R. Jung, M.J. Chrispeels, Plasma membrane intrinsic proteins from maize cluster in two sequence subgroups with differential aquaporin activity, Plant Physiology 122 (2000) 1025—1034.

[15] M. Moshelion, D. Becker, A. Biela, N. Uehlein, R. Hedrich, B. Otto, H. Levi, N. Moran, R. Kaldenhoff, Plasma membrane aquaporins in the motor cells of Samanea saman: diurnal and circadian regulation, Plant Cell 14 (2002) 727—739.

[16] K. Fetter, V. Van Wilder, M. Moshelion, F. Chaumont, Interactions between plasma membrane aquaporins modulate their water channel activity, Plant Cell 16 (2004) 215—228.

[17] C. Hachez, M. Moshelion, E. Zelazny, D. Cavez, F. Chaumont, Localization and quantification of plasma membrane aquaporin expression in maize primary root: a clue to understanding their role as cellular plumbers, Plant Molecular Biology 62 (2006) 305—323.

[18] C. Hachez, R.B. Heinen, X. Draye, F. Chaumont, The expression pattern of plasma membrane aquaporins in maize leaf highlights their role in hydraulic regulation, Plant Molecular Biology 68 (2008) 337—353.

[19] F. Siefritz, M.T. Tyree, C. Lovisolo, A. Schubert, R. Kaldenhoff, PIP1 plasma membrane aquaporins in tobacco: from cellular effects to function in plants, Plant Cell 14 (2002) 869—876.

[20] P. Martre, R. Morillon, F. Barrieu, G.B. North, P.S. Nobel, M.J. Chrispeels, Plasma membrane aquaporins play a significant role during recovery from water deficit, Plant Physiology 130 (2002) 2101—2110.

[21] T. Henzler, R.N. Waterhouse, A.J. Smyth, M. Carvajal, D.T. Cooke, A.R. Sch ffner, E. Steudle, D.T. Clarkson, Diurnal variations in hydraulic conductivity and root pressure can be correlated with the expression of putative aquaporins in the roots of Lotus japonicus, Planta 210 (1999) 50—60.

[22] F. Lopez, A. Bousser, I. Sissoeff, M. Gaspar, J. Lachaise, J. Hoarau, A. Mahe, Diurnal regulation of water transport and aquaporin gene expression in maize roots: contribution of PIP2 proteins, Plant and Cell Physiology 44 (2003) 1384—1395.

[23] R.K. Vandeleur, G. Mayo, M.C. Shelden, M. Gilliham, B.N. Kaiser, S.D. Tyerman, The role of plasma membrane intrinsic protein aquaporins in water transport through roots: diurnal and drought stress responses reveal different strategies between isohydric and anisohydric cultivars of grapevine, Plant Physiology 149 (2009) 445—460.

[24] H.L. Lian, X. Yu, D. Lane, W.N. Sun, Z.C. Tang, W.A. Su, Upland rice and lowland rice exhibited different PIP expression under water deficit and ABA treatment, Cell Research 16 (2006) 651—660.

[25] S.H. Lee, G.C. Chung, J.Y. Jang, S.J. Ahn, J.J. Zwiazek, Overexpression of PIP2;5 aquaporin alleviates effects of low root temperature on cell hydraulic conductivity and growth in Arabidopsis, Plant Physiology 159 (2012) 479—488.

[26] C. Hachez, D. Veselov, Q. Ye, H. Reinhardt, T. Knipfer, W. Fricke, F. Chaumont, Short-term control of maize cell and root water permeability through plasma membrane aquaporin isoforms, Plant, Cell & Environment 35 (2012) 185—198.

[27] W.H. Zhang, S.D. Tyerman, Inhibition of water channels by $HgCl_2$ in intact wheat root cells, Plant Physiology 120 (1999) 849—857.

[28] K.L. Forrest, M. Bhave, The PIP and TIP aquaporins in wheat form a large and diverse family with unique gene structures and functionally important features, Functional & Integrative Genomics 8 (2008) 115—133.

[29] J. Dubcovsky, J. Dvorak, Genome plasticity a key factor in the success of polyploid wheat under domestication, Science 316 (2007) 1862—1866.

[30] NBSC, China Statistical Yearbook 2011, China Statistics Press, Beijing, 2011.

[31] A.G. Condon, R.A. Richards, G.J. Rebetzke, G.D. Farquhar, Improving intrinsic water-use efficiency and crop yield, Crop Science 42 (2002) 122—131.

[32] Z.B. Zhang, L. Shan, Comparison study on water use efficiency of wheat flag leaf, Chinese Science Bulletin 43 (1998) 1205—1211.

[33] M.P. Reynolds, M. Balota, M.I.B. Delgado, I. Amani, R.A. Fischer, Physiological and morphological traits associated with spring wheat yield under hot, irrigated conditions, Australian Journal of Plant Physiology 21 (1994) 717—730.

[34] C.X. Zhao, X.P. Deng, L. Shan, E. Steudle, S.Q. Zhang, Q. Ye, Changes in root hydraulic conductivity during wheat evolution, Journal of Integrative Plant Biology 47 (2005) 302—310.

[35] W.R. Li, S.Q. Zhang, L. Shan, Effect of water stress on characteristics of root water uptake and photosynthesis in alfalfa seedlings, Acta Agrestia Sinica 15 (2007) 206—211.

[36] Z.X. Mu, S.Q. Zhang, A.H. Liang, Z.S. Liang, Relationship between maize root hydraulic conductivity and drought resistance, Acta Agronomica Sinica 31 (2005) 203—208.

[37] P.J. Franks, P.L. Drake, R.H. Froend, Anisohydric but isohydrodynamic: seasonally constant plant water potential gradient explained by a stomatal control mechanism incorporating variable plant hydraulic conductance, Plant, Cell & Environment 30 (2007) 19—30.

[38] E. Steudle, Pressure probe techniques: basic principles and application to studies of water and solute relations at the cell, tissue and organ level, in: J.A.C. Smith, H. Griffiths (Eds.), Water Deficits: Plant Responses from Cell to Community, Bios Scientific Publishers Ltd., Oxford, 1993, pp. 5—36.

[39] K.J. Livak, T.D. Schmittgen, Analysis of relative gene expression data using real-time quantitative PCR and the $2^{-\Delta\Delta Ct}$ method, Methods 25 (2001) 402—408.